

Unravelling High-Molecular-Weight DBP Toxicity Drivers in Chlorinated and Chloraminated Drinking Water: Effect-Directed Analysis of Molecular Weight Fractions

Huiyu Dong, Amy A. Cuthbertson, Michael J. Plewa, Chad R. Weisbrod, Amy M. McKenna, and Susan D. Richardson*



Cite This: <https://doi.org/10.1021/acs.est.3c00771>



Read Online

ACCESS |



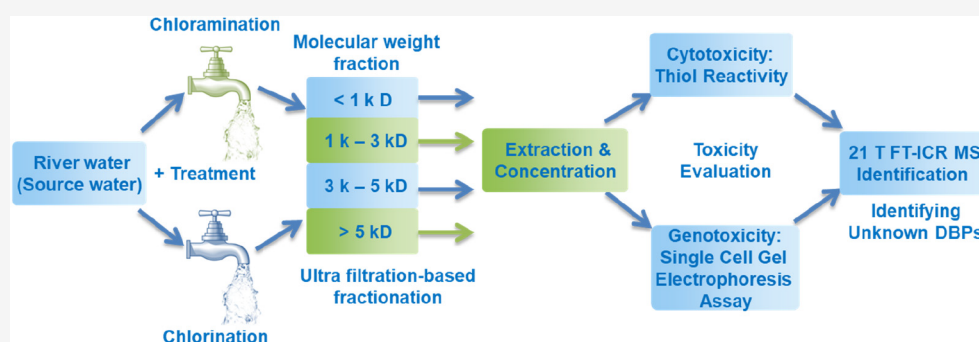
Metrics & More



Article Recommendations



Supporting Information



ABSTRACT: As disinfection byproducts (DBPs) are ubiquitous sources of chemical exposure in disinfected drinking water, identifying unknown DBPs, especially unknown drivers of toxicity, is one of the major challenges in the safe supply of drinking water. While >700 low-molecular-weight DBPs have been identified, the molecular composition of high-molecular-weight DBPs remains poorly understood. Moreover, due to the absence of chemical standards for most DBPs, it is difficult to assess toxicity contributions for new DBPs identified. Based on effect-directed analysis, this study combined predictive cytotoxicity and quantitative genotoxicity analyses and Fourier transform ion cyclotron resonance mass spectrometry (21 T FT-ICR-MS) identification to resolve molecular weight fractions that induce toxicity in chloraminated and chlorinated drinking waters, along with the molecular composition of these DBP drivers. Fractionation using ultrafiltration membranes allowed the investigation of <1 kD, 1–3 kD, 3–5 kD, and >5 kD molecular weight fractions. Thiol reactivity based predictive cytotoxicity and single-cell gel electrophoresis based genotoxicity assays revealed that the <1 kD fraction for both chloraminated and chlorinated waters exhibited the highest levels of predictive cytotoxicity and direct genotoxicity. The <1 kD target fraction was used for subsequent molecular composition identification. Ultrahigh-resolution MS identified singly charged species (as evidenced by the 1 Da spacing in ^{13}C isotopologues), including 3599 chlorine-containing DBPs in the <1 kD fraction with the empirical formulas CHOCl , CHOCl_2 , and CHOCl_3 , with a relative abundance order of $\text{CHOCl} > \text{CHOCl}_2 \gg \text{CHOCl}_3$. Interestingly, more high-molecular-weight CHOCl_{1-3} DBPs were identified in the chloraminated vs chlorinated waters. This may be due to slower reactions of NH_2Cl . Most of the DBPs formed in chloraminated waters were composed of high-molecular-weight Cl-DBPs (up to 1 kD) rather than known low-molecular-weight DBPs. Moreover, with the increase of chlorine number in the high-molecular-weight DBPs detected, the O/C ratio exhibited an increasing trend, while the modified aromaticity index (AI_{mod}) showed an opposite trend. In drinking water treatment processes, the removal of natural organic matter fractions with high O/C ratio and high AI_{mod} value should be strengthened to minimize the formation of known and unknown DBPs.

KEYWORDS: toxicity drivers, unknown DBPs, fractionation, high molecular weight, ultrafiltration

INTRODUCTION

Disinfection of drinking water is one of the ten public health achievements in the 20th century.¹ Various disinfectants, e.g., free chlorine, chloramine (NH_2Cl), chlorine dioxide (ClO_2), and ozone (O_3), can reduce the spread of waterborne diseases by inactivating pathogens in water.² The disinfectant simultaneously reacts with natural or anthropogenic organic matter and halides to form toxic disinfection byproducts

Special Issue: Oxidative Water Treatment: The Track Ahead

Received: January 30, 2023

Revised: May 6, 2023

Accepted: June 12, 2023

(DBPs), which are associated with the potential for adverse health conditions, including cancer and reproductive or developmental effects.³ To date, >700 DBPs have been identified, approximately 100 of which have been investigated for their occurrence, formation, and quantitative cytotoxicity and genotoxicity.^{3–5} However, >50% of the total organic halogen (TOX) formed during disinfection remains unknown.⁶ Due to the adverse health effects associated with DBPs in drinking water, the World Health Organization, United States, European Union, China, and other countries have currently set up guidelines or regulations for several DBPs in drinking water.^{7–9} For example, 11 DBPs including four trihalo-methanes (THMs) and five haloacetic acids (HAAs) have been regulated in the U.S. However, most DBPs are not yet adequately identified, regulated, or controlled in drinking water.⁷

As chloramination forms lower levels of regulated THMs and HAAs than chlorination, chloramine has been increasingly adopted as a secondary disinfectant to maintain a residual disinfection ability in distribution systems.^{10–12} However, TOX formed during chloramination (generally less than that from chlorination) can still reach considerable levels, depending on the chloramine dose, Cl/N ratio, pH, and other conditions.¹³ Moreover, in chloraminated drinking water, up to 70% of TOX formed remains unknown, a significantly higher unknown fraction than observed for chlorination (~50% of TOX unknown).^{14,15} The unknown TOX formed during chlorination and chloramination may contain a substantial amount of toxic DBPs, which need identification.^{16,17}

Continued efforts have been made to identify unknown DBPs in drinking water, especially for the toxicity drivers.^{18–28} The identification of unknown DBPs and corresponding toxicity assessments significantly enriched the knowledge of unknown TOX. One of the tricky challenges in the assessment of complex drinking water mixtures is the identification of those DBPs that contribute significantly to observed toxicity. A recent forcing factor study of U.S. drinking waters, which combined the quantification of 72 DBPs with whole-water cytotoxicity measurements, found unregulated dihaloacetonitriles to be the main cytotoxicity drivers in drinking water, along with iodo acids in chloraminated drinking waters containing iodide.²⁹ When measured whole-water toxicity data are not available, another approach called “TIC-Tox” is often used, where each measured low-molecular-weight DBP is multiplied by the reported cytotoxicity or genotoxicity index of that DBP measured in Chinese hamster ovary (CHO) cells.³⁰ However, the TIC-Tox method is limited to the ~100 low-molecular-weight known DBPs for which quantitative cellular toxicity data have been evaluated. For unknown/unquantified DBPs, it is difficult to use the TIC-Tox method to identify unknown DBP toxicity drivers.⁷

Although most DBPs previously identified through gas chromatography–mass spectrometry (GC-MS)-based methods are low-molecular-weight (one and two carbon atoms), volatile or semivolatile compounds, this does not necessarily mean that the majority of DBP toxicity drivers fall into this category. While >700 low-molecular-weight DBPs have been identified, the molecular composition of high-molecular-weight DBPs (>C₂) remains poorly understood.³¹ Liquid chromatography–mass spectrometry (LC-MS) based methods, using softer ionization methods (e.g., electrospray ionization (ESI)) and high-resolution MS (HRMS), have heightened the possibilities for the detection of unknown DBPs. With

increased use of LC-MS, more and more hydrophilic, high-molecular-weight DBPs have been identified, broadening our understanding of the physical and chemical characteristics of DBPs in drinking water.^{19,20,32,33}

With new DBPs and micropollutants increasingly being identified,³⁴ drinking water is known as a complex mixture comprised of thousands of compounds, which makes it nearly impossible to attribute drinking water toxicity to any one compound. Generally, natural organic matter (NOM) is the main precursor of DBPs in drinking water, the total concentration and characteristics of which are a function of allochthonous sources, autochthonous production, and other anthropogenic compounds.³⁵ As NOM is a heterogeneous mixture of organic chemicals with various polarities and molecular weights in an aquatic environment, DBPs formed during disinfection may exhibit the same trend, i.e., various polarities and molecular weights. Previous investigations have shown that nonvolatile DBPs are related to much of the total toxicity in drinking water.^{36–38} Therefore, the overall toxicity in drinking water may be driven by a few mixture fractions.³⁹ For the identification of unknown DBPs, it is helpful to switch from chemical-by-chemical identification to fraction identification, e.g., via linking chemical identification and toxicity analysis by trait-based or effect-directed approaches.

Identifying the toxicity-driver factors leading to dominant toxicity and subsequently removing these DBP precursors or minimizing DBP formation would reduce the health risks of the drinking water.⁴⁰ Effect-directed analysis (EDA), combining chemical analysis and toxicity/effect evaluation, is an efficient tool to identify key toxicants in complex water matrices. By a bioassay-directed fractionation of water samples, EDA can reduce natural water samples to less complex mixtures or individual compounds for identification of the relevant toxicity drivers.^{41–44} In EDA, *in vitro* toxicity assessment of different fractions is widely used to discover toxicity-driving fractions of bulk water. Although *in vitro* toxicity evaluation cannot guarantee a DBP to be a human health risk factor, these quantitative *in vitro* assays allow for quantitative comparisons of the relative cytotoxicity, genotoxicity, or toxicogenomic effects of a series of drinking water fractions.^{45–48} Then a subsequent HRMS analysis can be conducted to identify the DBP toxicity drivers in a less complex sample fraction. Currently, suspect screening and nontarget screening strategies have been applied to toxicant identification in EDA.⁴³ As unknown DBPs usually lack standard chemical and MS library information, a nontarget approach is more feasible for unveiling unknown DBPs present in these waters. For example, FT-ICR-MS has been used to determine the molecular formulas of chlorinated and brominated DBPs formed in drinking water samples.^{37,49} The ultrahigh mass-resolving power and mass accuracy of FT-ICR-MS allow confident assignments for tens of thousands of the unique elemental compositions possible.

Herein, the EDA protocol including predictive cytotoxicity and direct genotoxicity assays and nontarget identification using FT-ICR-MS was adopted to identify unknown DBP toxicity drivers in chlorinated and chloraminated drinking waters. More specifically, we aim to (1) evaluate toxicity-driven molecular weight fractions in chloraminated and chlorinated drinking water, (2) obtain molecular information on the unknown high-molecular-weight DBPs in toxicity-driven fractions, and (3) compare these high-molecular-weight DBPs in chlorinated and chloraminated drinking waters. To

the best of our knowledge, this work presents the first EDA-based nontarget analysis of unknown high-molecular-weight DBPs in finished drinking water.

METHODS

Reagents. Detailed reagent information can be found in [Text S1](#) (Supporting Information).

Water Sample Collection. Chlorinated and chloraminated drinking water (100 L each) were sampled from drinking water plants in Texas (TX), Georgia (GA), and South Carolina (SC) along with 20–100 L of source water (river water) that serves these plants. The two SC plants share a common source water (sample 3), with a midrange TOC and bromide/iodide ions; one plant uses pre-ClO₂ with NH₂Cl disinfection (sample 1), and the other plant uses Cl₂ disinfection (sample 2). The TX plant (sample 5) uses NH₂Cl disinfection and has a high TOC/high bromide/iodide ion source water (sample 4), and the GA plant uses Cl₂ disinfection (sample 7) and has a low TOC/low bromide/iodide ion source water (sample 6). Further information is shown in [Table S1](#), and water quality data and disinfectant doses are shown in [Table S2](#). 20 L Teflon bottles, rinsed three times before collection, were used to collect water samples, and no quencher was added to maintain the stability of formed DBPs.

Molecular Formula Identification Workflow. The workflow for unraveling high-molecular-weight DBP toxicity drivers in drinking waters is shown in [Figure S1](#). Briefly, water samples were size-fractionated using ultrafiltration membranes, extracted using XAD resins, and evaluated for predictive and genomic DNA damage. For the most cytotoxic and genotoxic fractions, FT-ICR-MS analysis was adopted to obtain molecular information.

Molecular Weight Fractionation and XAD Resin Extraction. Finished drinking water and source waters were fractionated using a Millipore Pellicon 2 mini ultrafiltration device (Amicon, Beverly, MA) with ultrafiltration membranes (molecular weight cutoffs of 500–5 kD), which resulted in several fractions with different effective molecular weights. 100 L of chloraminated drinking water (sample 1) was concentrated to ~50 mL in each molecular mass fraction, namely, >5, and 3–5, and 1–3 kD except for the <1 kD fraction. Further concentration was not carried out for the <1 kD fraction which had passed through all the ultrafiltration systems. The <0.5 kD fractionation is an inefficient process (only tried for sample 4), and was not applied to other samples. XAD resin extraction of finished whole drinking water (20 L) and molecular-weight-fractionated waters (100 L of total water fractionated) was carried out based on a published procedure.^{50,51} Briefly, drinking waters were added with sulfuric acid to adjust pH < 1 and passed over a resin bed of DAX-8 and XAD-2 resins (with a ratio of 770:1 water:resins used). Ethyl acetate was adopted to elute extracts from the resins, which was then dried with Na₂SO₄ and concentrated under N₂ using a TurboVap (Biotage) for toxicity analysis and nontarget analysis. Representative molecular-weight-based fractions of chloraminated and chlorinated drinking water samples are shown in [Figure S2](#).

Toxicity Assays. The organic solvent eluent of the resin was used for toxicity evaluation. As a widely used toxicity test method, concentration factor or equivalent water volume is adopted in dose–response curves.^{52–54} A *N*-acetyl-L-cysteine (NAC) thiol reactivity assay was employed for predictive cytotoxicity that measures the alkylation of cysteine thiol in

NAC to mimic the cysteine thiol in glutathione.⁵³ Glutathione is a cellular antioxidant which could prevent damage induced by toxic compounds. Thiol reactivity results correlate with CHO cell cytotoxicity in various waters (e.g., drinking water, surface water, and wastewater).^{12,53,55} Thus, thiol reactivity as a surrogate for cytotoxicity provides a screening assay to evaluate the toxicity of a drinking water sample. This predictive assay does not require cells or biological safety measures and can be used as a screening tool to identify the toxicity drivers in drinking water.^{53,55} This thiol reactivity assay was used to investigate cytotoxicity of drinking water fractions, and a CHO single-cell gel electrophoresis (SCGE) assay^{28,56} was used to evaluate the genotoxicity of different molecular weight fractions. Details on the thiol reactivity assay are provided in [Text S2](#) and were published,⁵³ and SCGE assay protocols are described in [Text S3](#) and were published.⁵

Nontarget Analysis of Unknown DBPs. Nontarget analysis of unknown DBPs was conducted at the National High Magnetic Field Laboratory (Tallahassee, FL), where a 21 T FT-ICR-MS with ESI ionization and resolving power of ≥1000000 was used to identify molecular information for unknown DBPs (*m/z* 50–1000).^{57,58} Prior to FT-ICR-MS analysis, an aliquot of each XAD extract (20–100 L) was solvent-exchanged with methanol (200 μL), followed by 2-fold dilution. Direct infusion was adopted to achieve longer acquisition times. A complete list of experimental details is included in [Text S4](#). All FT-ICR-MS files will be publicly available via the Open Science framework.

Molecular Formula Assignments. Only mass spectral peaks with signal magnitude >6-fold the baseline root-mean-square noise were exported to a peak list, converted and sorted based on Kendrick mass defect analysis, and assigned elemental compositions by PetroOrg software. During molecular formula assignments, errors >0.5 ppm were discarded, and only chemical classes with a combined relative abundance ≥0.25% of the total were further considered. The chlorine number and type of halogens in unknown DBPs were determined and verified based on characteristic isotopic patterns. As this study focuses on the identified chlorine-containing DBPs (i.e., CHOCl_{1–3}), the identified unknown DBPs are divided into three groups based on the number of chlorine atoms (i.e., CHOCl, CHOCl₂, and CHOCl₃), which has been widely adopted in previous publications.^{59,60} H/C and O/C ratios of individual molecular formulas identified were calculated to construct van Krevelen plots. Parameters of molecules, including average carbon oxidation state ($\overline{\text{OS}}_c$), double bond equivalents per carbon (DBE/C), and modified aromatic index (AI_{mod}) were calculated based on elemental compositions according to eqs 1–3 (*n* is the number of atoms of each type in the DBP molecular formula).⁶¹

$$\overline{\text{OS}}_c = -\frac{n\text{H} - (n\text{O} \times 2) - n\text{Cl}}{nC} \quad (1)$$

$$\text{DBE/C} = 1 + 0.5 \times \frac{(nC \times 2) - n\text{H} - n\text{Cl}}{nC} \quad (2)$$

$$\text{AI}_{\text{mod}} = \frac{1 + n\text{C} - 0.5 \times n\text{O} - 0.5 \times n\text{H} - 0.5 \times n\text{Cl}}{nC - 0.5 \times n\text{O}} \quad (3)$$

Target DBPs and Total Organic Halogen (TOX). 65 regulated and priority unregulated DBPs (all low molecular weight) from 8 DBP classes were also quantified for

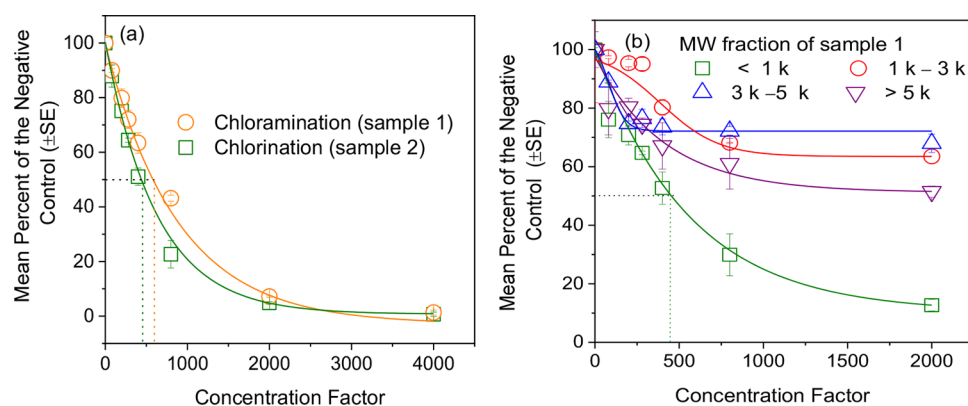


Figure 1. Thiol-reactivity-based cytotoxicity of chloraminated (sample 1 in SC) and chlorinated (sample 2 in SC) drinking waters (a) and thiol-reactivity-based cytotoxicity of molecular-weight-fractionated chloraminated drinking water (sample 1) (b). The dashed lines represent a schematic diagram of regression to obtain EC_{50} , and the error bars represent the standard error of the mean with triplicate/concentration.

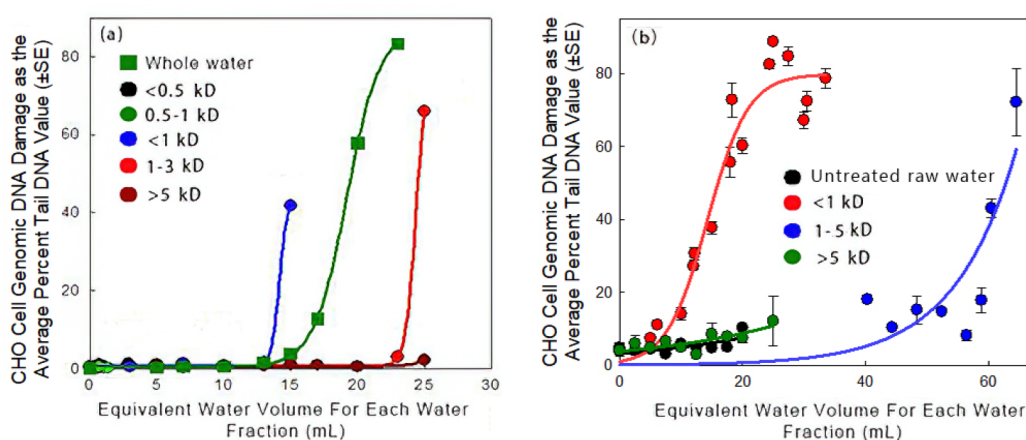


Figure 2. Molecular-weight-fractionated genotoxicity of chlorinated drinking water from GA (sample 7) (a) and river water and chloraminated drinking water from TX (samples 4 and 5, respectively) (b). In Figure 2a, the CHO cell genomic DNA damage was only observed in the <1 kD fraction, the 1–3 kD fraction, and the whole water samples. The <0.5 kD fraction, as well as the >5 kD fraction, were not genotoxic. The liter-equivalent is the volume of the original water sample that contains the mass of organic matter with which the cells were treated. Data from sample 7 should be considered preliminary, as only two replicates per concentration were able to be determined due to limited sample volume.

comparison using liquid–liquid extraction, derivatization, and GC-MS. Method details have been published and can be found in Text S5.^{29,62} 4 THMs, 6 iodinated trihalomethanes (I-THMs), 8 bromo/chloro haloacetic acids (Br/Cl-HAAs), 4 iodinated haloacetic acids (I-HAAs), 10 haloacetonitriles (HANs), 7 halonitromethanes (HNMs), 9 halo ketones (HKs), 13 haloacetamides (HAMs), and 4 trihaloacetaldehydes (tri-HALs) were included in the target DBP analysis. Speciated TOX (TOCl, TOBr, and TOI) was analyzed using combustion ion chromatography; details have been published and are provided in Text S6.²⁹

Statistical Analyses. For the toxicity analyses of each water sample, the lowest summed molar concentration that induced a statistically significant level of toxicity as compared to its concurrent negative control ($P \leq 0.05$) was determined by a one-way analysis of variance (ANOVA) test with the power of the ANOVA test maintained as >0.8 at $\alpha = 0.05$.⁶³ EC_{50} values (effective concentration of the sample that induced a reduction in NAC thiol concentration by 50% compared to negative controls) were determined by regression analysis.^{52,53} Like LC_{50} , EC_{50} can be used as an indicator of cytotoxicity of water samples. In this study, the higher the EC_{50} value, the higher the concentration factor required to induce a reduction

in NAC thiol concentration by 50%, indicating that the cytotoxicity of the water sample is relatively low. The mean and standard error (SE) of the mean for the EC_{50} values (thiol reactivity assay), the mean thiol reactivity index (TRI) (defined as $(EC_{50}^{-1}) (10^3)$), 50% Tail DNA values (genotoxicity assay), and genotoxicity index value (GTI) (defined as $(50\%TDNA^{-1}) (10^3)$) were determined for water samples using nonlinear regression and bootstrap statistical analysis.

RESULTS AND DISCUSSION

Toxicity Overview of Chlorinated and Chloraminated Drinking Waters. For the identification of unknown DBP toxicity drivers, multiple toxicity assays applied to the extracted chemical organics from a water sample are useful to identify toxic responses associated with water quality and the disinfection process.^{53,64,65} Then the water sample fractions expressing high levels of toxicity are candidates for detailed chemical identification using HRMS to uncover the toxic agents. The toxicity of chlorinated and chloraminated drinking water samples from SC were first analyzed using the thiol reactivity assay. Previously, we compared the TRI and cytotoxicity index (CTI) values for drinking water and pool

samples, and TRI and CTI were statistically significantly correlated ($r = 0.99$; $P < 0.001$).^{52,53} Thiol reactivity can be a reliable predictor of CHO cell cytotoxicity in water samples. Figure 1a shows that the TRI value of chlorinated water sample 1 is 1.3-fold that of the whole chloraminated sample 2, indicating that sample 1 is slightly more toxic than sample 2. Then, the TRI values of different MW fractions were investigated using a thiol reactivity assessment. As shown in Table S3, the EC₅₀ value of the chloraminated <1 kD fraction was much lower than those of the other three fractions, indicating that the <1 kD fraction is the most cytotoxic fraction.

SCGE is a sensitive assay which can quantitatively measure genomic DNA damage in individual nuclei of treated cells induced by a toxicant, which has been widely used as a predictor of carcinogenic activity.^{66,67} As shown in Figure 2, the <1 kD fraction exhibits potent mammalian cell genotoxicity in both the chlorinated and chloraminated drinking water samples collected from TX and GA. The SCGE genotoxic potency, calculated for each fraction as the midpoint in each concentration–response curve, revealed that the <1 kD fraction exhibited the highest genotoxicity for both chlorinated and chloraminated waters. In the chlorinated water sample, the <1 kD fraction exhibited genomic DNA damage similar to that of the whole water sample, indicating that the genotoxicity of the whole water sample may be mostly attributed to the <1 kD fraction. In the chloraminated drinking water sample, the <1 kD fraction was a more potent DNA-damaging fraction than the high-molecular-weight fraction (>1 kD), consistent with the thiol reactivity results. As shown in Table S4, the GTI of the <1 kD fraction was 4-fold more genotoxic than the 1–5 kD fraction of the chloraminated drinking water sample. Overall, the <1 kD fraction in both chloraminated and chlorinated drinking water samples is a potent mammalian cell cytotoxin and genotoxin, which may pose an adverse effect to public health and warrants a further chemical identification to determine their exact chemical compositions.

DBP Formation in Chlorinated and Chloraminated Drinking Waters. Total Organic Halogen (TOX) and Known DBPs. Generally, higher levels of TOX are useful indicators of higher levels of DBPs, including known and unknown DBPs in drinking water. The TOCl, TOBr, and TOI values of the chlorinated and chloraminated drinking water samples from SC (samples 1 and 2) were determined. TOCl dominated the overall DBP formation. As shown in Figure S3, TOCl and TOBr were 92.3 ± 2.4 and 20.7 ± 0.9 $\mu\text{g/L}$, respectively, in the chlorinated water sample, higher than those in the chloraminated water sample. However, the TOI of the chlorinated water sample (0.6 ± 0.1 $\mu\text{g/L}$) was slightly lower than that of the chloraminated water sample (0.9 ± 0.15 $\mu\text{g/L}$), probably due to higher levels of iodo-DBPs during chloramination, which generally occur due to competing reactions and different rates of formation.^{64,68} Kristiana et al. compared the formation of halogen-specific TOX from chlorination and chloramination of NOM isolates (molecular size fractions of NOM that were subsequently chlorinated or chloraminated) and found that THMs comprised only 7% of TOX in chloraminated water, while they comprised up to 47% of TOX in chlorinated water.¹⁵ Thus, the chlorinated high-molecular-weight unknown DBPs in these waters were a focus of subsequent nontarget identification.

Figure 3 illustrates the total concentrations ($\mu\text{g/L}$) of each DBP class in chlorinated and chloraminated drinking water

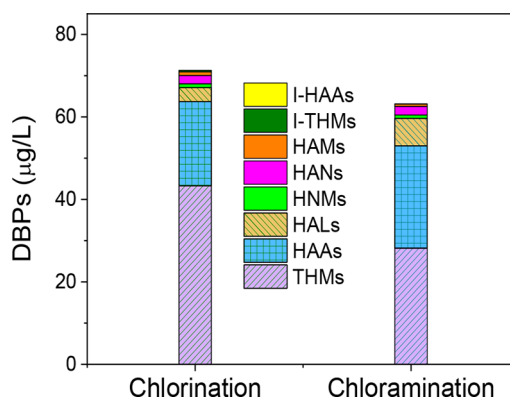


Figure 3. Quantified DBPs formed in chloraminated (sample 1 in SC) and chlorinated (sample 2 in SC) drinking waters. All DBP analyses were conducted in duplicate.

from SC. Eight DBP classes, including THMs, HAAs, HALs, HNMs, HANs, HAMS, I-THMs, and I-HAAs, were detected in both the chlorinated and chloraminated samples. Overall, the formation of known DBPs in chlorinated drinking water was higher than in chloraminated drinking water. THMs and HAAs are the most prevalent of the known DBPs in both the chlorinated and chloraminated drinking waters, with summed THM and HAA concentrations in the range of 28.5–42.3 and 21.4–32.1 $\mu\text{g/L}$, respectively (Figure 3). The third most abundant DBP group was HALs, with trichloroacetaldehyde (TCAL) being consistently detected at the highest concentration (up to 6.5 $\mu\text{g/L}$). Further, nitrogenous DBPs (HNMs, HANs, and HAMS) were also detected in water samples (<5.0 $\mu\text{g/L}$ for each group), indicating the presence of nitrogenous DBP precursors in the source water.

Unknown DBPs. The molecular formulas of chlorine-containing high-molecular-weight DBPs in the most toxic fraction (<1 kD) were analyzed using ultrahigh-resolution FT-ICR-MS. Because chlorine-containing contaminants can also occur in source waters, molecular formula crosschecking was conducted in the source vs disinfected waters to ensure that all assigned chlorinated formulas were DBPs formed during treatment. Figure S4 shows the negative-ion FT-ICR mass spectra of the chlorinated and chloraminated water extracts (samples 1 and 2) from SC. The majority of the peaks were in the m/z range of 150–1000, which are similar to those presented previously, with multiple peaks per nominal mass.^{37,69} The negative-ion FT-ICR mass spectra of the chloraminated and chlorinated water samples look similar, both of which generally follow a normal distribution. The ultrahigh resolution and mass accuracy of abundant peaks enabled the accurate assignment of a unique molecular composition to most peaks. For chlorine-containing DBP molecular formula identifications, isotopic pattern matching for one, two, and three chlorine-containing formulas were conducted one by one (Figure S5) to improve the accuracy of identification. The isotopic pattern matching for CHOC_2Cl , CHOC_2Cl_2 , and CHOC_2Cl_3 DBPs are exemplified in Figure 4 with three chlorine-containing DBPs (i.e., $\text{C}_{19}\text{H}_{24}\text{O}_8\text{Cl}$, $\text{C}_{11}\text{H}_5\text{O}_7\text{Cl}_2$, and $\text{C}_6\text{H}_2\text{O}_5\text{Cl}_3$).

Using FT-ICR-MS analysis, 3599 chlorine-containing DBPs ($S/N > 10$) were detected in these chloraminated and chlorinated water samples from SC, which fall into molecular formulas with $\text{CHOC}_1\text{--}3$ and masses ranging from 150 to 1000 D and are rich in carboxylic and phenolic groups. No

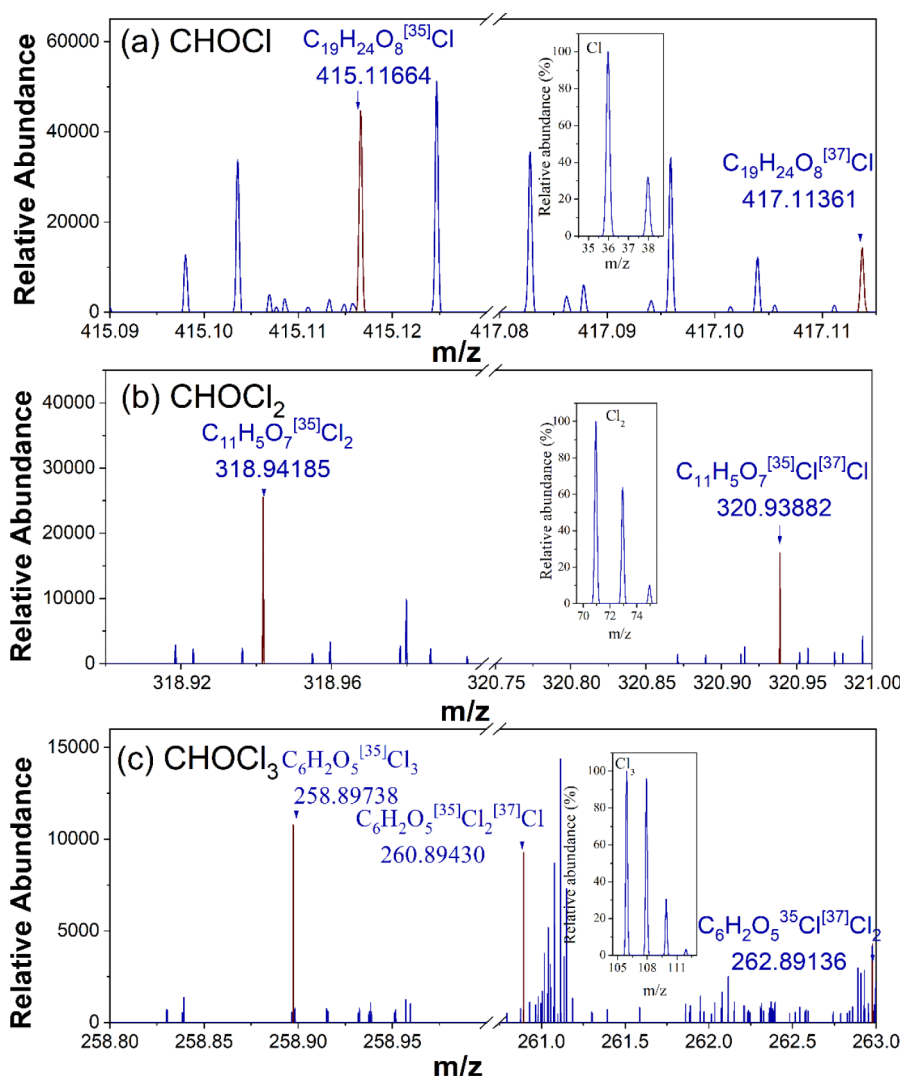


Figure 4. Isotopic pattern matching for high-molecular-weight CHOCI, CHOCI₂, and CHOCI₃ DBPs in the FT-ICR mass spectra of chloraminated drinking water (sample 1 in SC). Theoretical isotopic structures of CHOCI, CHOCI₂, and CHOCI₃ are shown for each isotopic peak. Δm values between masses calculated from the assigned isotopic composition with experimentally derived masses (FT-ICR-MS) are in the range of 11–25 ppb.

chlorine-containing nitrogenous or sulfur-containing products were identified, probably due to the relatively low abundance of nitrogenous and sulfur-containing precursor molecules. Given that known N-DBPs were formed (Figure 3), we would expect unknown high-molecular-weight N-DBPs to also form. At the same time, it is also possible that the reaction time of NOM with chloramine in drinking water treatment was sufficient to cause the high-molecular-weight N-DBPs to further transform into lower molecular weight N-DBPs. In addition, in the FT-ICR-MS analysis, only data with $S/N > 10$ were identified, indicating that the low-abundance CHONCl group may have been filtered out. Moreover, the negative ESI ionization mode may be unfavorable for CHON and CHONCl groups. Thus, these results might not fully present the presence of the CHON group and the formation of CHONCl DBPs. The identification of unknown N-DBPs needs further investigation in the future.

Of the Cl-DBPs, 1847 contained one chlorine (CHOCI), 1243 contained two chlorines (CHOCI₂), and 509 contained three chlorines (CHOCI₃). In our previous comprehensive review of DBPs, >600 Cl-DBPs were compiled (mostly

identified using GC-MS or derivatization with GC-MS), with 217 DBPs containing at least one chlorine atom.²⁴ Generally, GC-MS analysis (electron ionization) selects for the identification of somewhat nonpolar and (semi)volatile DBPs, while this study adopted ESI, which can provide complementary information to GC-MS and broaden insights into the composition of TOX in drinking water.

Earlier studies using FT-ICR-MS to identify unknown DBPs in drinking water (without toxicity) have found some empirical formulas of CHOCI, CHOCI₂, and CHOCI₃, but in much lower numbers compared to our findings. For example, 659 CHOCI and 348 CHOCI₂ DBPs were identified in chlorinated simulated drinking water from China.³⁷ Another full-scale chlorinated drinking water study using FT-ICR-MS reported 357 CHOCI and 199 CHOCI₂ DBPs.⁶⁹ In a study from Sweden, no CHOCI₃ molecular formula was observed for unknown DBPs in drinking water samples.⁷⁰ CHOCI₃ DBPs were speculated to form but further transform to known DBPs (e.g., volatile THMs), which are no longer amenable for FT-ICR-MS analysis.⁷⁰ For the first time, apart from CHOCI and CHOCI₂, up to 509 CHOCI₃ DBPs were successfully detected

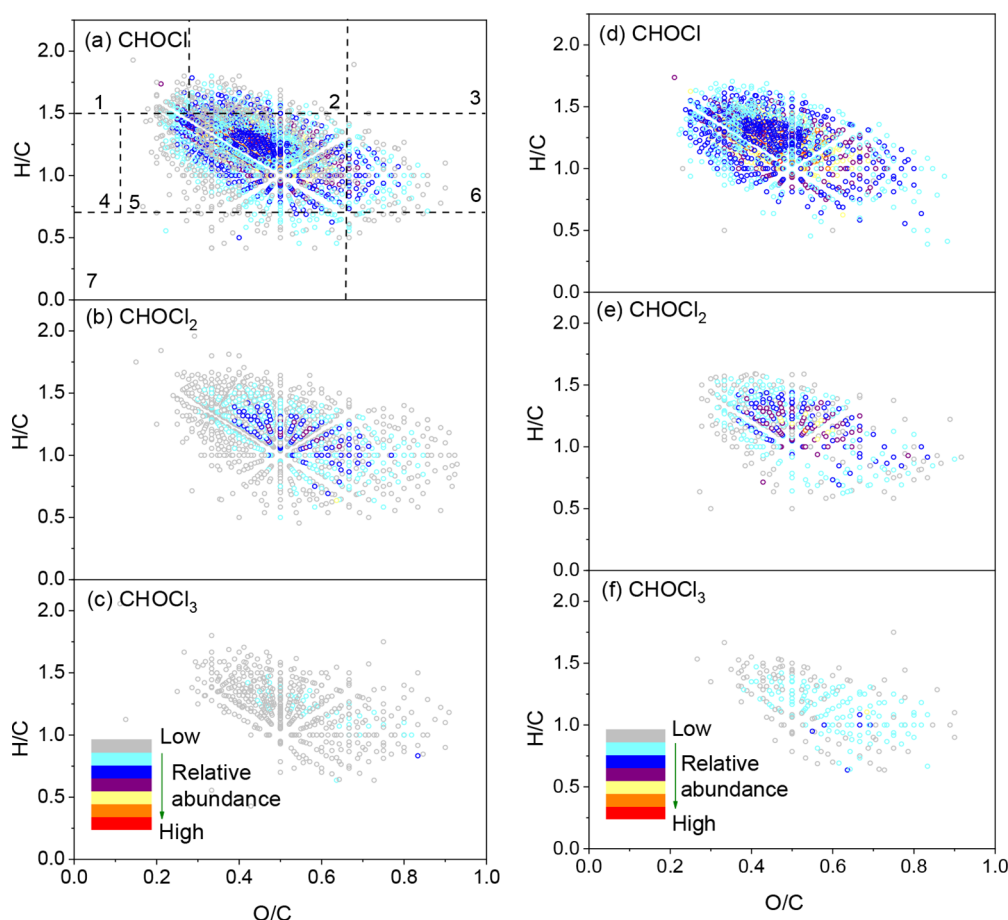


Figure 5. Van Krevelen plots of high-molecular-weight CHOCI , CHOCI_2 , and CHOCI_3 DBPs formed in chloraminated (a–c, sample 1 in SC) and chlorinated (d–f, sample 2 in SC) drinking water samples (<1 kD fraction). With the color of circles from gray to red, the relative abundance of DBPs increased in water samples. Regions 1–7 in Figure 5a indicate lipids (1), aliphatic/peptides (2), carbohydrates (3), unsaturated hydrocarbons (4), lignin/CRAM (carboxylic-rich aromatic moieties)-like (5), tannins (6), and aromatic structures (7).

in drinking water samples 1 and 2 in this study. Moreover, as the CHOCI_3 group may be key intermediates of known DBPs (e.g., THMs and HAAs usually containing 3 halogen atoms), the successful identification of CHOCI_3 DBPs may facilitate the determination of more specific formation pathways for regulated and unregulated, low-molecular-weight DBPs.

Interestingly, in this study, more Cl-DBPs were identified in chloraminated drinking water sample 1 than in chlorinated drinking water sample 2. Among the 3599 detected Cl-DBPs, 3423 (95%) were present in the chloraminated drinking water sample, with 1739 CHOCI , 1203 CHOCI_2 , and 481 CHOCI_3 DBPs, while in chlorinated drinking water sample, only 1092 CHOCI , 761 CHOCI_2 , and 302 CHOCI_3 DBPs were found. Because FT-ICR-MS reports tens of thousands of individual elemental compositions within a single sample, van Krevelen diagrams are often applied to DOM samples (and sometimes to DBP samples)⁷¹ to rapidly visualize compositional changes between samples.^{72,73} In the van Krevelen diagrams constructed for these size-fractionated drinking waters (Figure 5), each dot represents one or more elemental compositions with a specific O/C and H/C ratio. Based on different H/C and O/C ratios, the ranges of the classifications for the van Krevelen diagram can be classified into 7 groups, including lignin/carboxylic-rich aromatic moieties (lignin/CRAMs), lipids, carbohydrates, aliphatic/peptides, unsaturated hydrocarbons, tannins, and aromatic structures (Table S5).³⁶ Note that a van

Krevelen plot combines all isomers into a single O/C and H/C value, which can result in a loss of chemical specificity, meaning that two molecules that land on the same spot on a van Krevelen plot may react differently when exposed to the same disinfectant.⁷⁴

As shown in Figure 5, the van Krevelen diagrams for both the chlorinated and chloraminated drinking water samples were similar, with a dominance of lignin/CRAM-like formulas with an O/C molar ratio of 0.1–0.67 and a H/C molar ratio of 0.7–1.5. The lignin/CRAM-like region potentially includes carboxyl-rich alicyclic molecules, indicating that this fraction of DOM serves as the main precursors of CHOCI_{1-3} DBPs.⁷⁵ In addition, tannin-like formulas (region 6 in Figure 5a) also appear in both drinking water samples, which may be additional terrigenous precursors to CHOCI_{1-3} DBPs. Although condensed hydrocarbon (region 4) and aromatic structures (region 7) can be released into the water from incomplete combustion of forest/grass or fossil fuel in the watershed,⁷¹ few chlorinated DBPs were identified in regions 4 and 7, indicating that the NOM reactivity of these regions during chlorination and chloramination were lower than those of lignin/CRAM-like and tannin-like regions. Interestingly, with the increase of chlorine atoms, the distribution pattern of CHOCI_{1-3} exhibits a shift, i.e., from a dominant lignin/CRAM-like region to a dominant tannin-like pattern, indicating that the tannin-like region of NOM (higher O/C

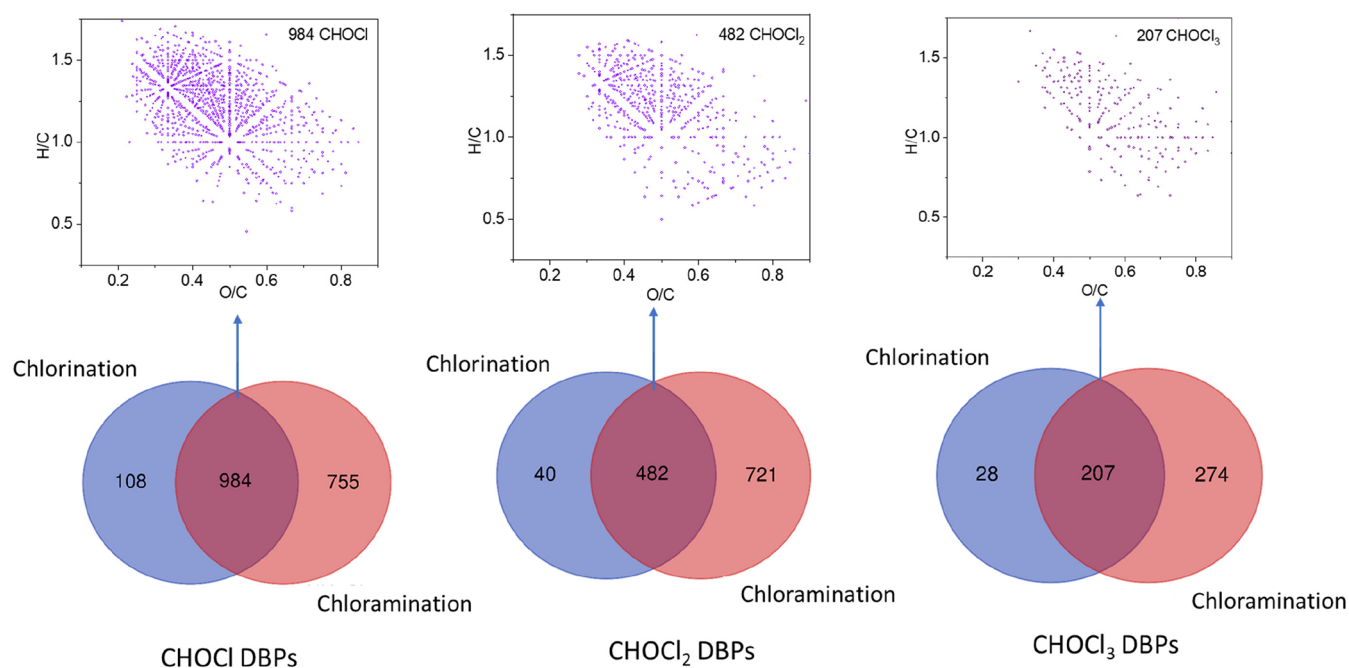


Figure 6. Overlap of high-molecular-weight CHOCl, CHOCl₂, and CHOCl₃ DBPs formed in both chloraminated (sample 1 in SC) and chlorinated (sample 2 in SC) drinking water samples (<1 kD fraction).

ratios) is prone to serve as precursors of multichlorine-containing DBPs.

FT-ICR-MS can be used for semiquantitative analysis using the peak intensities of different molecular species in a mass spectrum to estimate their relative concentrations, rather than providing absolute quantification. Figure S6 shows a representative negative-ion ESI-FT-ICR mass spectrum for chlorine-containing products at nominal m/z 375. In the mass range of m/z 375.0–375.05, 70% of the ions have been assigned with molecular formulas and 50% of the peaks were identified to be chlorine-containing DBPs. It seems that the relative abundance of the CHOCl group was higher than that of the CHOCl₂ group. Then the relative abundances of CHOCl, CHOCl₂, and CHOCl₃ DBPs in the chloraminated drinking water sample 1 were statistically analyzed using a box-whisker plot (Figure S7). It is clear that the relative abundance followed the order CHOCl > CHOCl₂ > CHOCl₃, which is reasonable, as CHOCl₂ and CHOCl₃ groups were formed from the CHOCl group. Moreover, the chlorination reaction rate of activated aromatic structures (e.g., electrophilic aromatic substitution reactions with phenolic compounds) usually decreases after each chlorine incorporation, meaning that the 3 chlorine atom incorporation into the CHO moiety may be a slow process during the continuous chlorination.⁷⁶ Thus, for the high-molecular-weight DBPs, the relative abundance and compound types of CHOCl DBPs were significantly higher than those of CHOCl₂ and CHOCl₃ DBPs. However, it should be noted that the relative abundance of ESI peaks is not directly equivalent to their concentrations, as both matrix effects and ion suppression can occur, which affect quantitative analysis.⁷⁷

To further illustrate the unknown DBP formation mechanism and precursors, the O/C and H/C ratios of identified chlorinated DBPs (i.e., CHOCl, CHOCl₂, and CHOCl₃) were compared with the CHO group (Figure S8). For the O/C ratio, significant differences were observed between CHO and CHOCl, CHOCl₂, and CHOCl₃ groups (P

< 0.001) in both chloraminated and chlorinated drinking water samples. This result is consistent with the van Krevelen diagrams in Figure 5, indicating that the newly formed chlorine-containing components (CHOCl, CHOCl₂, and CHOCl₃) are more oxidized than the already present CHO group. Meanwhile, the CHOCl₃ DBPs identified in this study have relatively high O/C ratios, indicating that the CHOCl₃ group may be rich in carboxylic and phenolic groups and the chlorination of NOM was preferred to precursors that have high O/C ratios. In contrast, the difference of H/C among CHOCl, CHOCl₂, and CHOCl₃ DBPs was not significant. Only in chloraminated drinking water samples was the H/C ratio of CHOCl_{1–3} higher than that of the CHO group (P < 0.01). \overline{OS}_c vs double bond equivalence (DBE)/C of CHOCl, CHOCl₂, and CHOCl₃ DBPs are plotted in Figure S9. Consistent with the previous results, CHOCl₃ DBPs exhibit higher \overline{OS}_c and lower DBE/C than CHOCl and CHOCl₂ DBPs. It is not surprising that the \overline{OS}_c values of CHOCl₃ were the highest among the 3-chlorine-containing group because chlorination of NOM both through electrophilic substitution and addition to unsaturated bonds usually leads to an increase in the average \overline{OS}_c .

During the chlorination process, oxidation, electrophilic substitution, and addition reactions with NOM are possible pathways and both addition and electrophilic substitution reactions can induce the formation of chlorinated DBPs. In chlorine addition reactions, addition of $\delta^+Cl-OH\delta^-$ to double bonds could increase H/C and O/C, while in electrophilic substitution reactions, a hydrogen atom is usually displaced by chlorine, leading to a decreased H/C and unaffected O/C.⁷⁶ Overall, the O/C ratios increased, while H/C ratios were mostly unchanged compared with the CHO group in chloraminated drinking water samples, indicating that the internal averaging of both the substitution reactions and the addition reactions determined the O/C and H/C ratios in the CHOCl, CHOCl₂, and CHOCl₃ groups.

Figure 6 exhibits the overlap of CHOCl , CHOCl_2 , and CHOCl_3 DBPs formed in both the chloraminated and chlorinated water samples using Venn diagrams, which shows not only the unique DBPs for chlorination and chloramination but also the common DBPs that have identical molecular formulas formed in both disinfection processes. The CHOCl formulas identified in both chlorinated and chloraminated drinking water samples were very similar. Most of the CHOCl (90%), CHOCl_2 (63%), and CHOCl_3 (69%) DBPs formed in chlorination were also detected in chloramination, while the overlaps of chlorinated DBPs account for only $\sim 60\%$, 40% , and 40% of CHOCl , CHOCl_2 , and CHOCl_3 , respectively. As these chlorinated and chloraminated drinking waters share a common source water, the precursors of CHOCl_{1-3} DBPs should be quite similar and the molecular diversity of CHOCl_{1-3} DBPs could reflect how the disinfectants (i.e., HOCl and NH_2Cl) impact the formation of TOX and DBPs. Of the different chloramination reaction mechanisms, DBPs formed during reactions between HOCl hydrolyzed from monochloramine and NOM, are mostly the same as those produced in chlorination.⁷⁸ However, as the hydrolysis of NH_2Cl into HOCl is a slow process, DBPs from chloramination may be comprised of chlorinated high-molecular-weight DBPs ($>C_2$), rather than known low-molecular-weight DBPs (C_1 and C_2).

A previous study found that there are good linear correlations between the formation of TOX and the aromatic character of the NOM isolates, with aromatic moieties playing an important role in the formation of TOX.¹⁵ A modified aromaticity index (AI_{mod}), an indicator for the identification of aromatic and polycyclic fractions in NOM, was adopted and calculated from the molecular formulas to estimate the fraction of aromatic and condensed aromatic structures.⁷⁹ As shown in eq 3, AI_{mod} only counts half of the oxygen atoms and assumes the other half is σ bonded. Two threshold values are set for the existence of either aromatic ($\text{AI}_{\text{mod}} > 0.5$) or condensed aromatic structures ($\text{AI}_{\text{mod}} \geq 0.67$) in NOM.⁷⁹ As shown in Figure S10, most AI_{mod} values of CHOCl , CHOCl_2 , and CHOCl_3 groups are <0.5 in both the chloraminated and chlorinated drinking water samples. In the chloraminated water sample, 89% of CHOCl , 91% of CHOCl_2 , and 94% of CHOCl_3 have AI_{mod} values <0.5 . These AI_{mod} distributions indicate that few CHOCl , CHOCl_2 , and CHOCl_3 DBPs belong to chlorinated aromatic or condensed aromatic structures. With the increase of chlorine atoms, the AI_{mod} values of CHOCl , CHOCl_2 , and CHOCl_3 groups exhibit a decreasing trend. For example, the average AI_{mod} values of CHOCl , CHOCl_2 , and CHOCl_3 in chloraminated drinking water were determined to be 0.29 ± 0.16 , 0.28 ± 0.15 , and 0.26 ± 0.14 , respectively. The reaction pathway between chlorine and aromatic structures has been investigated intensely.^{76,80} As the number of chlorine atoms increases in high-molecular-weight DBPs, AI_{mod} shows a downward trend, indicating that the partial structure of the NOM is undergoing transformation from aromatic to aliphatic, which eventually leads to the formation of low-molecular-weight DBPs.

Chlorine-Free Groups Identified in Drinking Water Samples. Apart from the CHOCl , CHOCl_2 , and CHOCl_3 groups, chlorine-free groups including CHO, CHON, and CHOS groups were detected in both the chloraminated and chlorinated drinking water samples. Taking chloraminated water sample 1 as an example, 3265 CHO, 1772 CHON, and 958 CHOS formulas were identified in the <1 kD fraction

(Figure S11). Compared with the CHO group of raw water (sample 8) in Figure S12, a low O/C ratio fraction was removed during the coagulation-sedimentation-filtration treatment. Similar with identified CHOCl_{1-3} DBPs, most of the CHO, CHON, and CHOS formulas are in the lignin/CRAM-like region of a van Krevelen plot. The relative abundance followed the order $\text{CHO} \gg \text{CHON} > \text{CHOS}$. In aquatic NOM, CHO is the dominant composition, while nitrogen primarily exists in amide or amino-quinone structures and heterocyclic nitrogen structures.⁸¹ The presence of sulfur compounds (i.e., CHOS) in the drinking water samples is also not surprising. Sulfur-containing compounds have been identified in NOM using negative ionization FT-ICR-MS.⁸² In this study, given that nitrogenous DBPs including HAMS, HNMs, and HANs have been detected in chlorinated and chloraminated drinking water, it is speculated that unknown nitrogenous DBPs (like CHONCl_{1-3}) would form after disinfection. However, due to the low abundance of CHON and CHOS groups (i.e., precursors of DBPs), it is difficult to conduct isotopic verification for chlorinated CHON and CHOS formulas, especially for ^{37}Cl -containing formulas. Generally, known nitrogenous DBPs exhibit significantly higher cytotoxicity and genotoxicity than carbonaceous DBPs that do not contain nitrogen.^{5,54,83} Therefore, it is important to identify unknown nitrogenous DBPs and determine their formation mechanisms and pathways. Continued research is necessary to improve the ionization and enrichment efficiency of nitrogenous and sulfur-containing compounds, and to further identify their unknown chlorinated products.

ENVIRONMENTAL IMPLICATIONS

DBPs pose a ubiquitous source of chemical exposure in drinking water. While >700 DBPs (mostly C_1 or C_2) have been identified in drinking water, the composition of high-molecular-weight DBPs in drinking waters, especially for the toxicity-driven unknown DBPs, remain poorly understood. Due to the wide absence of chemical standards, it is usually impossible to assess the toxicity contribution of identified DBPs by HRMS. This study combined toxicity analysis and FT-ICR-MS chemical analysis to identify the toxicity-driven high-molecular-weight DBPs in drinking water. Using a thiol-reactivity-based predictive cytotoxicity and direct genotoxicity assay, the <1 kD fraction in both the chloraminated and chlorinated water drinking samples exhibited the highest levels of cytotoxicity and genotoxicity. The most toxic fractions were identified by FT-ICR-MS, with 1847 CHOCl , 1243 CHOCl_2 , and 509 CHOCl_3 DBPs being successfully identified (according to molecular formulas). With the increase of chlorine number in the unknown CHOCl_{1-3} DBPs, O/C exhibited an increasing trend, while AI_{mod} showed an opposite trend. Unexpectedly, more unknown CHOCl_{1-3} DBPs were identified in the chloraminated drinking water. Due to slow hydrolysis (to HOCl) and the weak oxidation ability of NH_2Cl , most DBPs formed in the chloraminated drinking water sample may be composed of chlorine-containing unknown DBPs rather than known THMs and HAAs (Figure S13). To minimize the formation of known and unknown DBPs, removal of the NOM fractions with high O/C ratio and high AI_{mod} values should be included in drinking water treatment processes.⁸⁴ Overall, all the reaction mechanisms (oxidation, electrophilic substitution, addition reactions), ion suppression within the ESI source, and internal averaging could impact the results. More control experiments are necessary in the future to

unveil the formation mechanism of unknown toxicity-driven DBPs.

■ ASSOCIATED CONTENT

SI Supporting Information

The Supporting Information is available free of charge at <https://pubs.acs.org/doi/10.1021/acs.est.3c00771>.

Additional details on reagent information, procedures for known DBP analysis, for total organic halogen analysis, for thiol reactivity assay, and for single cell gel electrophoresis, water sample information, genotoxicity statistical analysis, classifications for the van Krevelen diagram, EDA workflow, photo of molecular weight fraction extracts, procedures for single-cell gel electrophoresis assay, TOX results, FT-ICR mass spectra, theoretical isotopic structures, relative abundance of unknown DBPs, O/C and H/C ratios, oxidation state analysis, modified aromaticity index analysis, CHO, CHON, and CHOS groups, and formation mechanism and pathways of Cl-DBPs, with accompanying texts, tables, and figures (PDF)

■ AUTHOR INFORMATION

Corresponding Author

Susan D. Richardson – Department of Chemistry and Biochemistry, University of South Carolina, Columbia, South Carolina 29208, United States; orcid.org/0000-0001-6207-4513; Phone: +1-803-777-6932; Email: richardson.susan@sc.edu

Authors

Huiyu Dong – Department of Chemistry and Biochemistry, University of South Carolina, Columbia, South Carolina 29208, United States; Key Laboratory of Drinking Water Science and Technology, Research Center for Eco-Environmental Sciences, Beijing 100085, People's Republic of China; orcid.org/0000-0002-5955-6228

Amy A. Cuthbertson – Department of Chemistry and Biochemistry, University of South Carolina, Columbia, South Carolina 29208, United States

Michael J. Plewa – Department of Crop Sciences, University of Illinois at Urbana–Champaign, Urbana, Illinois 61801, United States; orcid.org/0000-0001-8307-1629

Chad R. Weisbrod – National High Magnetic Field Laboratory, Florida State University, Tallahassee, Florida 32310, United States; orcid.org/0000-0001-5324-4525

Amy M. McKenna – National High Magnetic Field Laboratory, Florida State University, Tallahassee, Florida 32310, United States; Department of Soil and Crop Sciences, Colorado State University, Fort Collins, Colorado 80523, United States; orcid.org/0000-0001-7213-521X

Complete contact information is available at: <https://pubs.acs.org/doi/10.1021/acs.est.3c00771>

Notes

The authors declare no competing financial interest.

■ ACKNOWLEDGMENTS

We thank Gene Crumley for assistance with collecting some of the ultrafiltration fractions. The authors acknowledge funding from the National Science Foundation (CBET 1705206 and 1706862) and support from the National Natural Science

Foundation of China (52070184, 52270012), as well as the University of South Carolina for the purchase of an ultrafiltration device under an ASPIRE grant. A portion of this work was performed in the Ion Cyclotron Resonance user facility at the National High Magnetic Field Laboratory in Tallahassee, Florida, which is supported by the National Science Foundation Division of Materials Research and Division of Chemistry through DMR-1644779 and the State of Florida.

■ REFERENCES

- (1) Otterstetter, H.; Craun, G. Disinfection in the Americas: A Necessity. *J. - Am. Water Works Assoc.* **1997**, *89*, 8–10.
- (2) Calderon, R. L. The Epidemiology of Chemical Contaminants of Drinking Water. *Food Chem. Toxicol.* **2000**, *38*, S13–S20.
- (3) Richardson, S. D.; Plewa, M. J.; Wagner, E. D.; Schoeny, R.; DeMarini, D. M. Occurrence, Genotoxicity, and Carcinogenicity of Regulated and Emerging Disinfection By-products in Drinking Water: a Review and Roadmap for Research. *Mutat. Res-Rev. Mutat.* **2007**, *636*, 178–242.
- (4) Duirk, S. E.; Lindell, C.; Cornelison, C. C.; Kormos, J.; Ternes, T. A.; Attene-Ramos, M.; Osiol, J.; Wagner, E. D.; Plewa, M. J.; Richardson, S. D. Formation of Toxic Iodinated Disinfection By-products from Compounds Used in Medical Imaging. *Environ. Sci. Technol.* **2011**, *45*, 6845–6854.
- (5) Wagner, E. D.; Plewa, M. J. CHO Cell Cytotoxicity and Genotoxicity Analyses of Disinfection By-products: an Updated Review. *J. Environ. Sci.* **2017**, *58*, 64–76.
- (6) Han, J.; Zhang, X.; Jiang, J.; Li, W. How Much of the Total Organic Halogen and Developmental Toxicity of Chlorinated Drinking Water Might Be Attributed to Aromatic Halogenated DBPs? *Environ. Sci. Technol.* **2021**, *55*, 5906–5916.
- (7) Richardson, S. D.; Plewa, M. J. To Regulate or not to Regulate? What to do with More Toxic Disinfection By-products? *J. Environ. Chem. Eng.* **2020**, *8*, 103939.
- (8) World Health Organization (WHO). *Guidelines for Drinking-Water Quality*, 4th ed.; WHO: 2011.
- (9) EUR-Lex, Directive (EU) 2020/2184 of the European Parliament and of the Council on the Quality of Water Intended for Human Consumption. Available online: <https://eur-lex.europa.eu/legal-content/EN/TXT/HTML/?uri=CELEX:32020L2184&from=EN> (accessed on 28 January 2023).
- (10) Seidel, C. J.; McGuire, M. J.; Summers, R. S.; Via, S. Have Utilities Switched to Chloramines? *J. - Am. Water Works Assoc.* **2005**, *97*, 87–97.
- (11) Shah, A. D.; Krasner, S. W.; Lee, C. F. T.; von Gunten, U.; Mitch, W. A. Trade-Offs in Disinfection Byproduct Formation Associated with Precursor Preoxidation for Control of N-Nitrosodimethylamine Formation. *Environ. Sci. Technol.* **2012**, *46*, 4809–4818.
- (12) Li, X. F.; Mitch, W. A. Drinking Water Disinfection Byproducts (DBPs) and Human Health Effects: Multidisciplinary Challenges and Opportunities. *Environ. Sci. Technol.* **2018**, *52*, 1681–1689.
- (13) Diehl, A. C.; Speitel, G. E., Jr.; Symons, J. M.; Krasner, S. W.; Hwang, C. J.; Barrett, S. E. DBP Formation during Chloramination. *J. - Am. Water Works Assoc.* **2000**, *92*, 76–90.
- (14) Hua, G.; Reckhow, D. A. Comparison of Disinfection Byproduct Formation from Chlorine and Alternative Disinfectants. *Water Res.* **2007**, *41*, 1667–1678.
- (15) Kristiana, I.; Gallard, H.; Joll, C.; Croué, J.-P. The Formation of Halogen-specific TOX from Chlorination and Chloramination of Natural Organic Matter Isolates. *Water Res.* **2009**, *43*, 4177–4186.
- (16) Smith, E. M.; Plewa, M. J.; Lindell, C. L.; Richardson, S. D.; Mitch, W. A. Comparison of Byproduct Formation in Waters Treated with Chlorine and Iodine: Relevance to Point-of-use Treatment. *Environ. Sci. Technol.* **2010**, *44*, 8446–8452.
- (17) Cuthbertson, A. A.; Kimura, S. Y.; Liberatore, H. K.; Summers, R. S.; Knappe, D. R. U.; Stanford, B. D.; Maness, J. C.; Mulhern, R. E.;

- Selbes, M.; Richardson, S. D. Does Granular Activated Carbon with Chlorination Produce Safer Drinking Water? From Disinfection Byproducts and Total Organic Halogen to Calculated Toxicity. *Environ. Sci. Technol.* **2019**, *53*, 5987–5999.
- (18) Li, J.; Aziz, M. T.; Granger, C. O.; Richardson, S. D. Halocyclopentadienes: An Emerging Class of Toxic DBPs in Chlor(am)inated Drinking Water. *Environ. Sci. Technol.* **2022**, *56*, 11387–11397.
- (19) Zhai, H.; Zhang, X. Formation and Decomposition of New and Unknown Polar Brominated Disinfection Byproducts during Chlorination. *Environ. Sci. Technol.* **2011**, *45*, 2194–2201.
- (20) Yang, M. T.; Zhang, X. R. Comparative Developmental Toxicity of New Aromatic Halogenated DBPs in a Chlorinated Saline Sewage Effluent to the Marine Polychaete *Platynereis Dumerilii*. *Environ. Sci. Technol.* **2013**, *47*, 10868–10876.
- (21) Huang, R.; Wang, W.; Qian, Y.; Boyd, J. M.; Zhao, Y.; Li, X.-F. Ultra Pressure Liquid Chromatography-Negative Electrospray Ionization Mass Spectrometry Determination of Twelve Halobenzoquinones at ng/L Levels in Drinking Water. *Anal. Chem.* **2013**, *85*, 4520–4529.
- (22) Liberatore, H. K.; Plewa, M. J.; Wagner, E. D.; VanBriesen, J. M.; Burnett, D. B.; Cizmas, L. H.; Richardson, S. D. Identification and Comparative Mammalian Cell Cytotoxicity of New Iodo-phenolic Disinfection Byproducts in Chloraminated Oil and Gas Wastewaters. *Environ. Sci. Technol.* **2017**, *4*, 475–480.
- (23) Jeong, C. H.; Wagner, E. D.; Siebert, V. R.; Anduri, S.; Richardson, S. D.; Daiber, E. J.; McKague, A. B.; Kogevinas, M.; Villanueva, C. M.; Goslan, E. H.; Luo, W.; Isabelle, L. M.; Pankow, J. F.; Grazuleviciene, R.; Cordier, S.; Edwards, S. C.; Righi, E.; Nieuwenhuijsen, M. J.; Plewa, M. J. Occurrence and Toxicity of Disinfection Byproducts in European Drinking Waters in Relation with the HIWATE Epidemiology Study. *Environ. Sci. Technol.* **2012**, *46*, 12120–12128.
- (24) Richardson, S. D. Disinfection By-products: Formation and Occurrence of Drinking water. In *The Encyclopedia of Environmental Health*; Nriagu, J. O. Ed.; Elsevier: 2011; Vol. 2, pp 110–136.
- (25) Richardson, S. D.; Postigo, C. Discovery of New Emerging DBPs by High Resolution Mass Spectrometry. *Comprehensive Analytical Chemistry: Applications of TOF and Orbitrap MS in Environmental, Food, Doping, and Forensic Analysis*; Elsevier: Amsterdam, 2016; pp 335–356.
- (26) Postigo, C.; Cojocariu, C. I.; Richardson, S. D.; Silcock, P. J.; Barcelo, D. Characterization of Iodinated Disinfection By-products in Chlorinated and Chloraminated Waters Using Orbitrap Based Gas Chromatography-mass Spectrometry. *Anal. Bioanal. Chem.* **2016**, *408*, 3401–3411.
- (27) Plewa, M. J.; Wagner, E. D.; Richardson, S. D.; Thruston, A. D.; Woo, Y.-T.; McKague, A. B. Chemical and Biological Characterization of Newly Discovered Iodoacid Drinking Water Disinfection By-products. *Environ. Sci. Technol.* **2004**, *38*, 4713–4722.
- (28) Plewa, M. J.; Wagner, E. D.; Jazwierska, P.; Richardson, S. D.; Chen, P. H.; McKague, A. B. Halonitromethane Drinking Water Disinfection Byproducts: Chemical Characterization and Mammalian Cell Cytotoxicity and Genotoxicity. *Environ. Sci. Technol.* **2004**, *38*, 62–68.
- (29) Allen, J. M.; Plewa, M. J.; Wagner, E. D.; Wei, X.; Bokenkamp, K.; Hur, K.; Jia, A.; Liberatore, H. K.; Lee, C.-F. T.; Shirkhani, R.; Krasner, S. W.; Richardson, S. D. Drivers of Disinfection Byproduct Cytotoxicity in U.S. Drinking Water: Should Other DBPs be Considered for Regulation? *Environ. Sci. Technol.* **2022**, *56*, 392–402.
- (30) Plewa, M. J.; Wagner, E. D.; Richardson, S. D. TIC-Tox: A Preliminary Discussion on Identifying the Forcing Agents of DBP-mediated Toxicity of Disinfected Water. *J. Environ. Sci.* **2017**, *58*, 208–216.
- (31) Mitch, W. A.; Richardson, S. D.; Zhang, X.; Gonsior, M. High-molecular-weight By-products of Chlorine Disinfection. *Nature Water* **2023**, *1*, 336–347.
- (32) Liberatore, H. K.; Westerman, D. C.; Allen, J. M.; Plewa, M. J.; Wagner, E. D.; McKenna, A. M.; Weisbrod, C. R.; McCord, J. P.; Liberatore, R. J.; Burnett, D. B.; Cizmas, L.; Richardson, S. D. High-Resolution Mass Spectrometry Identification of Novel Surfactant-Derived Sulfur-Containing Disinfection By-Products from Gas Extraction Wastewater. *Environ. Sci. Technol.* **2020**, *54*, 9374–9386.
- (33) Ding, G. Y.; Zhang, X. R. A Picture of Polar Iodinated Disinfection Byproducts in Drinking Water by (UPLC/ESI-tqMS). *Environ. Sci. Technol.* **2009**, *43*, 9287–9293.
- (34) Richardson, S. D.; Kimura, S. Y. Water analysis: Emerging contaminants and current issues. *Anal. Chem.* **2020**, *92*, 473–505.
- (35) Amy, G. L.; Thompson, J. M.; Tan, L.; Davis, M. K.; Krasner, S. W. Evaluation of THM Precursor Contributions from Agricultural Drains. *J. - Am. Water Works Assoc.* **1990**, *82*, 57–64.
- (36) Harris, B. D.; Brown, T. A.; McGehee, J. L.; Houserova, D.; Jackson, B. A.; Buchel, B. C.; Krajewski, L. C.; Whelton, A. J.; Stenson, A. C. Characterization of Disinfection By-Products from Chromatographically Isolated NOM through High-Resolution Mass Spectrometry. *Environ. Sci. Technol.* **2015**, *49*, 14239–14248.
- (37) Zhang, H.; Zhang, Y.; Shi, Q.; Hu, J.; Chu, M.; Yu, J.; Yang, M. Study on Transformation of Natural Organic Matter in Source Water during Chlorination and Its Chlorinated Products using Ultrahigh Resolution Mass Spectrometry. *Environ. Sci. Technol.* **2012**, *46*, 4396–4402.
- (38) Gonsior, M.; Schmitt-Kopplin, P.; Stavkint, H.; Richardson, S. D.; Hertkorn, N.; Bastviken, D. Changes in Dissolved Organic Matter during the Treatment Processes of a Drinking Water Plant in Sweden and Formation of Previously Unknown Disinfection Byproducts. *Environ. Sci. Technol.* **2014**, *48*, 12714–12722.
- (39) Altenburger, R.; Walter, H.; Grote, M. What Contributes to the Combined Effect of a Complex Mixture? *Environ. Sci. Technol.* **2004**, *38*, 6353–6362.
- (40) Wawryk, N. J. P.; Craven, C. B.; Blackstock, L. K. J.; Li, X.-F. New Methods for Identification of Disinfection Byproducts of Toxicological Relevance: Progress and Future Directions. *J. Environ. Sci.* **2021**, *99*, 151–159.
- (41) Brack, W.; Schmitt-Jansen, M.; Machala, M.; Brix, R.; Barcelo, D.; Schymanski, E.; Streck, G.; Schulze, T. How to Confirm Identified Toxicants in Effect-directed Analysis. *Anal. Bioanal. Chem.* **2008**, *390*, 1959–1973.
- (42) Plewa, M. J.; Wagner, E. D. Charting a New Path to Resolve the Adverse Health Effects of DBPs. *Recent Advances in Disinfection By-Products*; American Chemical Society: 2015; ACS Symposium Series 1190, pp 3–23.
- (43) Guo, J.; Shen, Y.; Zhang, X.; Lin, D.; Xia, P.; Song, M.; Yan, L.; Zhong, W.; Gou, X.; Wang, C.; Wei, S.; Yu, H.; Shi, W. Effect-Directed Analysis Based on the Reduced Human Transcriptome (RHT) to Identify Organic Contaminants in Source and Tap Waters along the Yangtze River. *Environ. Sci. Technol.* **2022**, *56*, 7840–7852.
- (44) Escher, B. I.; Allinson, M.; Altenburger, R.; Bain, P. A.; Balaguer, P.; Busch, W.; Crago, J.; Denslow, N. D.; Dopp, E.; Hilscherova, K.; Humpage, A. R.; Kumar, A.; Grimaldi, M.; Jayasinghe, B. S.; Jarosova, B.; Jia, A.; Makarov, S.; Maruya, K. A.; Medvedev, A.; Mehinto, A. C.; Mendez, J. E.; Poulsen, A.; Prochazka, E.; Richard, J.; Schifferli, A.; Schlenk, D.; Scholz, S.; Shiraiishi, F.; Snyder, S.; Su, G.; Tang, J. Y. M.; Burg, B. v. d.; Linden, S. C. v. d.; Werner, I.; Westerheide, S. D.; Wong, C. K. C.; Yang, M.; Yeung, B. H. Y.; Zhang, X.; Leusch, F. D. L. Benchmarking Organic Micropollutants in Wastewater, Recycled Water and Drinking Water with In Vitro Bioassays. *Environ. Sci. Technol.* **2014**, *48*, 1940–1956.
- (45) Attene-Ramos, M. S.; Wagner, E. D.; Plewa, M. J. Comparative Human Cell Toxicogenomic Analysis of Monohaloacetic Acid Drinking Water Disinfection Byproducts. *Environ. Sci. Technol.* **2010**, *44*, 7206–7212.
- (46) Pals, J.; Attene-Ramos, M. S.; Xia, M.; Wagner, E. D.; Plewa, M. J. Human Cell Toxicogenomic Analysis Linking Reactive Oxygen Species to the Toxicity of Monohaloacetic Acid Drinking Water Disinfection Byproducts. *Environ. Sci. Technol.* **2013**, *47*, 12514–12523.

- (47) Lau, S. S.; Bokenkamp, K.; Tecza, A.; Wagner, E. D.; Plewa, M. J.; Mitch, W. A. Toxicological Assessment of Potable Reuse and Conventional Drinking Waters. *Nature Sustain.* **2023**, *6*, 39–46.
- (48) Li, X.-F.; Mitch, W. A. Drinking water disinfection byproducts (DBPs) and human health effects: multidisciplinary challenges and opportunities. *Environ. Sci. Technol.* **2018**, *52*, 1681–1689.
- (49) Lavonen, E. E.; Gonsior, M.; Tranvik, L. J.; Schmitt-Kopplin, P.; Kohler, S. J. Selective Chlorination of Natural Organic Matter: Identification of Previously Unknown Disinfection Byproducts. *Environ. Sci. Technol.* **2013**, *47*, 2264–2271.
- (50) Richardson, S. D. *XAD Resin Extraction of Disinfection By-Products in Drinking Water: SOP - RSB-003.1 - Revision No. 1*. U.S. Environmental Protection Agency: 2011.
- (51) Liao, X.; Allen, J. M.; Granger, C. O.; Richardson, S. D. How Well Does XAD Resin Extraction Recover Halogenated Disinfection Byproducts for Comprehensive Identification and Toxicity Testing? *J. Environ. Sci.* **2022**, *117*, 264–275.
- (52) Allen, J. M.; Plewa, M. J.; Wagner, E. D.; Wei, X.; Bollar, G. E.; Quirk, L. E.; Liberatore, H. K.; Richardson, S. D. Making Swimming Pools Safer: Does Copper-Silver Ionization with Chlorine Lower the Toxicity and Disinfection Byproduct Formation? *Environ. Sci. Technol.* **2021**, *55*, 2908–2918.
- (53) Dong, S.; Page, M. A.; Wagner, E. D.; Plewa, M. J. Thiol Reactivity Analyses To Predict Mammalian Cell Cytotoxicity of Water Samples. *Environ. Sci. Technol.* **2018**, *52*, 8822–8829.
- (54) Wei, X.; Yang, M.; Zhu, Q.; Wagner, E. D.; Plewa, M. J. Comparative Quantitative Toxicology and QSAR Modeling of the Haloacetonitriles: Forcing Agents of Water Disinfection Byproduct Toxicity. *Environ. Sci. Technol.* **2020**, *54*, 8909–8918.
- (55) Pals, J. A.; Wagner, E. D.; Plewa, M. J. Energy of the Lowest Unoccupied Molecular Orbital, Thiol Reactivity, and Toxicity of Three Monobrominated Water Disinfection Byproducts. *Environ. Sci. Technol.* **2016**, *50*, 3215–3221.
- (56) Wagner, E. D.; Plewa, M. J. Microplate-based Comet Assay. In *The Comet Assay in Toxicology*; Royal Society of Chemistry: London, 2009; pp 79–97.
- (57) Hendrickson, C. L.; Quinn, J. P.; Kaiser, N. K.; Smith, D. F.; Blakney, G. T.; Chen, T.; Marshall, A. G.; Weisbrod, C. R.; Beu, S. C. 21 T Fourier Transform Ion Cyclotron Resonance Mass Spectrometer: A National Resource for Ultrahigh Resolution Mass Analysis. *J. Am. Soc. Mass Spectrom.* **2015**, *26*, 1626–1632.
- (58) Smith, D. F.; Podgorski, D. C.; Rodgers, R. P.; Blakney, G. T.; Hendrickson, C. L. 21 T FT-ICR Mass Spectrometer for Ultrahigh-Resolution Analysis of Complex Organic Mixtures. *Anal. Chem.* **2018**, *90*, 2041–2047.
- (59) Prasert, T.; Ishii, Y.; Kurisu, F.; Musikavong, C.; Phungsai, P. Characterization of Lower Phong River Dissolved Organic Matters and Formations of Unknown Chlorine Dioxide and Chlorine Disinfection by-products by Orbitrap Mass Spectrometry. *Chemosphere* **2021**, *265*, 128653.
- (60) Chantarasrisuriyawong, T.; Prasert, T.; Yuthawong, V.; Phungsai, P. Changes in Molecular Dissolved Organic Matter and Disinfection by-product Formation during Granular Activated Carbon Filtration by Unknown Screening Analysis with Orbitrap Mass Spectrometry. *Water Res.* **2022**, *211*, 118039.
- (61) Kroll, J. H.; Donahue, N. M.; Jimenez, J. L.; Kessler, S. H.; Canagaratna, M. R.; Wilson, K. R.; Altieri, K. E.; Mazzoleni, L. R.; Wozniak, A. S.; Bluhm, H.; Mysak, E. R.; Smith, J. D.; Kolb, C. E.; Worsnop, D. R. Carbon Oxidation State as a Metric for Describing the Chemistry of Atmospheric Organic Aerosol. *Nature Chem.* **2011**, *3*, 133–139.
- (62) Cuthbertson, A. A.; Liberatore, H. K.; Kimura, S. Y.; Allen, J. M.; Bensussan, A. V.; Richardson, S. D. Trace Analysis of 61 Emerging Br-, Cl-, and I-DBPs: New Methods to Achieve Part-per-trillion Quantification in Drinking Water. *Anal. Chem.* **2020**, *92*, 3058–3068.
- (63) Box, G. E. P.; Hunter, W. G.; Hunter, J. S. *Statistics for Experimenters: An Introduction to Design, Data Analysis, and Model Building*; Wiley: 1978.
- (64) Richardson, S. D.; Fasano, F.; Ellington, J. J.; Crumley, F. G.; Buettner, K. M.; Evans, J. J.; Blount, B. C.; Silva, L. K.; Waite, T. J.; Luther, G. W.; McKague, A. B.; Miltner, R. J.; Wagner, E. D.; Plewa, M. J. Occurrence and Mammalian Cell Toxicity of Iodinated Disinfection Byproducts in Drinking Water. *Environ. Sci. Technol.* **2008**, *42*, 8330–8338.
- (65) Yang, Y.; Komaki, Y.; Kimura, S. Y.; Hu, H.-Y.; Wagner, E. D.; Marinas, B. J.; Plewa, M. J. Toxic Impact of Bromide and Iodide on Drinking Water Disinfected with Chlorine or Chloramines. *Environ. Sci. Technol.* **2014**, *48*, 12362–12369.
- (66) Lacoste, S.; Castonguay, A.; Drouin, R. Repair Kinetics of Specific Types of Nitroso-induced DNA Damage using the Comet Assay in Human Cells. *Mutat. Res., Rev. Mutat. Res.* **2007**, *624*, 18–30.
- (67) Komaki, Y.; Pals, J.; Wagner, E. D.; Mariñas, B. J.; Plewa, M. J. Mammalian Cell DNA Damage and Repair Kinetics of Monohaloacetic Acid Drinking Water Disinfection By-Products. *Environ. Sci. Technol.* **2009**, *43*, 8437–8442.
- (68) Bichsel, Y.; von Gunten, U. Formation of Iodo-trihalomethanes during Disinfection and Oxidation of Iodide-containing Waters. *Environ. Sci. Technol.* **2000**, *34*, 2784–2791.
- (69) Zhang, H.; Zhang, Y.; Shi, Q.; Ren, S.; Yu, J.; Ji, F.; Luo, W.; Yang, M. Characterization of Low Molecular Weight Dissolved Natural Organic Matter along the Treatment Trait of a Waterworks using Fourier Transform Ion Cyclotron Resonance Mass Spectrometry. *Water Res.* **2012**, *46*, 5197–5204.
- (70) Andersson, A.; Harir, M.; Gonsior, M.; Hertkorn, N.; Schmitt-Kopplin, P.; Kylin, H.; Karlsson, S.; Ashiq, M. J.; Lavonen, E.; Nilsson, K.; Pettersson, A.; Stavklint, H.; Bastviken, D. Waterworks-specific Composition of Drinking Water Disinfection By-products. *Environ. Sci. Water Res. Technol.* **2019**, *5*, 861–872.
- (71) Minor, E. C.; Steinbring, C. J.; Longnecker, K.; Kujawinski, E. B. Characterization of Dissolved Organic Matter in Lake Superior and its Watershed using Ultrahigh Resolution Mass Spectrometry. *Org. Geochem.* **2012**, *43*, 1–11.
- (72) van Krevelen, D. W. Graphical-statistical Method for the Study of Structure and Reaction Processes of Coal. *Fuel* **1950**, *29*, 269–284.
- (73) Kim, S.; Kramer, R. W.; Hatcher, P. G. Graphical Method for Analysis of Ultrahigh-Resolution Broadband Mass Spectra of Natural Organic Matter, the Van Krevelen Diagram. *Anal. Chem.* **2003**, *75*, 5336–5344.
- (74) Kim, S.; Kramer, R. W.; Hatcher, P. G. Graphical Method for Analysis of Ultrahigh-Resolution Broadband Mass Spectra of Natural Organic Matter, the Van Krevelen Diagram. *Anal. Chem.* **2003**, *75*, 5336–5344.
- (75) Hertkorn, N.; Benner, R.; Frommberger, M.; Schmitt-Kopplin, P.; Witt, M.; Kaiser, K.; Kettrup, A.; Hedges, J. I. Characterization of a Major Refractory Component of Marine Dissolved Organic Matter. *Geochim. Cosmochim. Acta* **2006**, *70*, 2990–3010.
- (76) Deborde, M.; von Gunten, U. Reactions of Chlorine with Inorganic and Organic Compounds during Water Treatment-Kinetics and Mechanisms: A Critical Review. *Water Res.* **2008**, *42*, 13–51.
- (77) Gan, S.; Guo, P.; Wu, Y.; Zhao, Y. A Novel Method for Unraveling the Black Box of Dissolved Organic Matter in Soils by FT-ICR-MS Coupled with Induction-Based Nanospray Ionization. *Environ. Sci. Tech. Lett.* **2021**, *8*, 356.
- (78) Vikesland, P. J.; Ozekin, K.; Valentine, R. L. Effect of Natural Organic Matter on Monochloramine Decomposition: Pathway Elucidation through the Use of Mass and Redox Balances. *Environ. Sci. Technol.* **1998**, *32*, 1409–1416.
- (79) Koch, B. P.; Dittmar, T. From Mass to Structure: an Aromaticity Index for High-resolution Mass Data of Natural Organic Matter. *Rapid Commun. Mass Spectrom.* **2006**, *20*, 926–932.
- (80) Gallard, H.; von Gunten, U. Chlorination of Phenols: Kinetics and Formation of Chloroform. *Environ. Sci. Technol.* **2002**, *36*, 884–890.
- (81) Thorn, K. A.; Cox, L. G. N-15 NMR Spectra of Naturally Abundant Nitrogen in Soil and Aquatic Natural Organic Matter Samples of the International Humic Substances Society. *Org. Geochem.* **2009**, *40*, 484–499.

(82) Wang, X.; Wang, J.; Li, K.; Zhang, H.; Yang, M. Molecular Characterization of Effluent Organic Matter in Secondary Effluent and Reclaimed Water: Comparison to Natural Organic Matter in Source Water. *J. Environ. Sci.* **2018**, *63*, 140–146.

(83) Plewa, M. J.; Wagner, E. D.; Muellner, M. G.; Hsu, K. M.; Richardson, S. D. Comparative Mammalian Cell Toxicity of N-DBPs and C-DBPs. In *Disinfection By-Products in Drinking Water: Occurrence, Formation, Health Effects, and Control*; American Chemical Society: 2008; ACS Symposium Series 995, pp 36–50.

(84) Ike, I. A.; Lee, Y.; Hur, J. Impacts of Advanced Oxidation Processes on Disinfection byproducts from Dissolved Organic Matter upon Post-chlor(am)ination: A Critical Review. *Chem. Eng. J.* **2019**, *375*, 121929.